

# Revisiting the deuteron mass radius via near-threshold $\rho^0$ , $\omega$ and $\phi$ meson photoproduction

Xiaoxuan Lin,<sup>1,2</sup> Wei Kou,<sup>1,3</sup> Shixin Fu,<sup>1,3</sup> Rong Wang,<sup>1,3,4</sup> Chengdong Han,<sup>1,3,4,\*</sup> and Xurong Chen<sup>1,3,4,5,†</sup>

<sup>1</sup>*Institute of Modern Physics, Chinese Academy of Sciences, Lanzhou 730000, China*

<sup>2</sup>*College of Physics Science and Technology, Hebei University, Baoding 71002, China*

<sup>3</sup>*School of Nuclear Science and Technology, University of Chinese Academy of Sciences, Beijing 100049, China*

<sup>4</sup>*State Key Laboratory of Heavy Ion Science and Technology,*

*Institute of Modern Physics, Chinese Academy of Sciences, Lanzhou 730000, China*

<sup>5</sup>*Southern Center for Nuclear Science Theory, Institute of Modern Physics,  
Chinese Academy of Sciences, Huizhou 516000, China*

We present a comprehensive analysis of the near-threshold photoproduction of the  $\rho^0$ ,  $\omega$ , and  $\phi$  mesons on a deuterium target, leveraging published datasets from the DESY and SLAC facilities. In our extraction of the deuteron mass radius, we employ a dipole-form scalar gravitational form factor to effectively model the  $|t|$ -dependence of the differential cross sections associated with vector meson photoproductions. Utilizing the vector-meson dominance model alongside a low-energy Quantum Chromodynamics (QCD) theorem assumption, we derive the deuteron mass radius from the near-threshold photoproduction data of the  $\rho^0$ ,  $\omega$ , and  $\phi$  mesons. The mass radii obtained from various datasets demonstrate consistency within the statistical uncertainties, yielding an average value of  $2.07 \pm 0.15$  fm. This precision surpasses previous estimates solely based on the  $\phi$  meson photoproduction data. Our findings provide novel constraints for theoretical nuclear structure models and significantly enhance our understanding of the mass distribution within the deuteron.

## I. INTRODUCTION

The size of proton, usually referred to as charge radius, magnetic radius, or mass radius, has always been a subject of heated discussions. Due to the differences in proton charge radius observed in high-precision measurements, the study of proton radius has always been the focal point of theoretical and experimental research, which is often referred to as the proton charge radius puzzle [1–3]. The nucleon magnetic radius [4–6] is a fundamental parameter that characterizes the spatial distribution of nucleon magnetization, which originates from the motion and intrinsic magnetic moment of its constituent quarks and gluons. The mass radius of nucleon describes the spatial distribution of mass within the nucleon, characterized by the mass density distribution. As a fundamental property of composite systems, the mass radius spans a vast range of scales, from subatomic particles in high-energy physics to galaxies in astrophysics. Recently, significant progress has been made in the determination and interpretation of nucleon and light-nuclei mass radii using various experimental and theoretical approaches [7–11]. The mass of a particle can be regarded as the response of the particle to the external gravitational field, and the gravitational form factor (GFF) of a particle is defined as the off-forward matrix element of the energy-momentum tensor (EMT) in the particle state [8, 12–15]. At low energy, the photoproduction of a quarkonium off the particle is connected to the scalar GFF of the particle,

which is sensitive to the particle mass distribution from the QCD trace anomaly.

Experimentally, the form factor  $F(q)$  of the target is measured as a function of the momentum transfer  $q$  in the low momentum elastic scattering process, and represents the Fourier transform of the density distributions  $\rho(r)$ , which provides crucial insights into the internal structure of the nucleon as described by QCD. The form factor enables researcher to access information about internal energy-momentum distributions inside the particle, thus directly linking experimental observables to fundamental QCD predictions [16]. For different hadronic systems, the internal density distribution is different, which corresponds to different form factor parameterizations and root-mean-square radius of the particle. Specifically, this mass radius provides insights into the mass density distribution within nuclear systems, directly linked to underlying quark and gluon dynamics [17, 18]. The experimental determination of the proton and deuteron charge radii has also received renewed attention from facilities worldwide, including experiments using electron-proton and electron-deuteron scattering, muonic atoms spectroscopy, and vector meson photoproduction processes [19–21]. Similarly, understanding the deuteron mass radius, which describes the mass distribution within the deuteron, is essential for deepening our knowledge of the structure of the atomic nucleus. Notably, recent analyses of vector meson photoproduction near production threshold have demonstrated their capability as sensitive probes for extracting nuclear mass distributions and radii. Currently, based on some vector meson near-threshold photoproduction data, people have done several works on extracting the mass radii of nucleon and light-nuclei [7–11].

\* chdhan@impcas.ac.cn (Corresponding Author)

† xchen@impcas.ac.cn (Corresponding Author)

In this work, we systematically investigate the mass radius of the deuteron by analyzing the momentum transfer ( $|t|$ ) dependence of differential cross sections from near-threshold photoproduction of the vector mesons  $\omega$ ,  $\rho^0$ , and  $\phi$ . By combining careful experimental data analysis with rigorous theoretical modeling, we aim to provide reliable results contributing to the ongoing development of nuclear structure physics and QCD phenomenology. The organization of this paper is as follows: Section II briefly introduces the GFF and mass radius; Section III presents the data analysis and results; At the end, a short summary is given in Section IV.

## II. GRAVITATIONAL FORM FACTOR AND MASS RADIUS

In a nonrelativistic and weak gravitational field approximation, the scalar GFF provides a useful framework for describing a particle mass distribution. That is, the mass radius of a particle can be theoretically defined in terms of the scalar GFF  $G(t = q^2)$ , the form factor of the trace of the QCD EMT instead of the form factor of  $T_{00}$  [8]. GFF can be obtained via the measurement of generalized parton distributions (GPDs) from various exclusive scattering processes, as their second Mellin moments yield the combinations of GFFs [14, 15]. In this study, a possible approach is to transform the study of graviton-nucleon scattering into the scalar GFF of the nucleon under the theoretical framework of the vector meson dominated (VMD) model. For a continuous mass density distribution at small momentum transfer  $t = q^2$ , the root-mean-square (RMS) radius of the nucleon is directly related to the slope of the scalar GFF at zero momentum transfer ( $t = 0$ ), expressed by [8, 22, 23],

$$\langle R_m^2 \rangle = 6 \frac{dG(t)}{dt} \Big|_{t=0}, \quad (1)$$

where the scalar GFF is normalized to  $G(0) = M$  at zero momentum transfer  $t = 0$ .

For this analysis, the VMD model was used for describing near-threshold photoproduction processes of vector mesons on nuclear targets. And the VMD model has been successfully applied in light vector meson near-threshold photoproductions studies [24–29], accurately linking measurable differential cross sections to the internal mass distributions of nucleon and light-nuclei [7–11, 30], as well as the vector-meson nucleon scattering lengths [24–29], etc. Specifically, at energies near the photoproduction threshold and at small momentum transfer ( $|t| \ll 1 \text{ GeV}^2$ ), the VMD model approximates the differential cross section by relating it directly to the square of the scalar GFF [8, 9]. The differential cross section for quarkonium near-threshold photoproduction processes in the small  $-|t|$  region can be described with

the scalar GFF, as shown below,

$$\frac{d\sigma}{dt} \propto G^2(t). \quad (2)$$

The validity of using the above equation to describe the photoproduction of light vector mesons off the nucleon or the hadronic matter is understandable. Brodsky *et al.* [31] demonstrate that in the small momentum transfer regime, the distinctive features of forward differential cross section for any possible vector meson leptonproduction can be reasonably factorized in perturbative QCD based on the  $q\bar{q}$  wave function of the vector meson and the target gluon distribution.

The dipole form factor from exponential distribution well describes the form factor of the nucleon within a wide kinematical range. To quantitatively describe the  $t$ -dependence of the experimental data and subsequently extract the deuteron mass radius, we adopt a widely-used dipole form parameterization for the scalar GFF [8, 9], which is written as,

$$G(t) = \frac{M}{(1 - t/m_s^2)^2}, \quad (3)$$

where  $m_s$  is dipole parameter determined from fitting differential cross-section data. This simple and effective parameterization has demonstrated its ability to reliably reproduce experimental differential cross sections across multiple vector meson photoproduction channels [9].

## III. DATA ANALYSIS AND RESULTS

### A. Photoproduction of $\rho^0$ on deuteron

The ABHBM collaboration [32] have been investigated the photoproduction of  $\rho^0$  differential cross section in a deuterium bubble chamber experiment at DESY with a bremsstrahlung beam at energies between 1 and 5 GeV. We analyzed near-threshold  $\rho^0$  meson photoproduction differential cross-section data on the deuterium target at  $E_\gamma = 1.8\text{--}2.5 \text{ GeV}$ . Two different resonance reconstruction models were considered, the Model (i) employs the standard Breit-Wigner resonance profile, while Model (ii) incorporates the interference effects from Drell-type one-pion exchange. Fig. 1 shows the differential cross sections  $d\sigma/dt$  of  $\rho^0$  meson photonproductions as a function of  $-t$ . Differential cross sections were independently fitted for each model to extract the corresponding deuteron mass radius, and from ABHBM data we extract the deuteron mass radii to be  $2.52 \pm 0.47 \text{ fm}$  (Model i) and  $2.23 \pm 0.33 \text{ fm}$  (Model ii), respectively. The extracted values of the dipole parameter  $m_s$  and deuteron radius  $\sqrt{\langle R_m^2 \rangle}$  are listed in Table I. The averaged deuteron mass radius of the two extracted values with different models is calculated to be  $2.33 \pm 0.27 \text{ fm}$ . We used the following formula for the calculation of weighted average:  $\bar{x} \pm \delta\bar{x} =$

Model	$E_\gamma$ (GeV)	$m_s$ (GeV)	$\sqrt{\langle R_m^2 \rangle}$ (fm)
(i)	1.8–2.5	$0.27 \pm 0.05$	$2.52 \pm 0.47$
(ii)	1.8–2.5	$0.31 \pm 0.05$	$2.23 \pm 0.33$

TABLE I. The extracted values of the dipole parameter  $m_s$  and deuteron mass radius  $\sqrt{\langle R_m^2 \rangle}$  from the differential cross sections of  $\rho^0$  photoproduction near threshold with different models at  $E_\gamma=1.8\text{--}2.5$  GeV, extrapolated to  $t = 0$  GeV<sup>2</sup>.

$\sum_i w_i x_i / \sum_i w_i \pm (\sum_i w_i)^{-1/2}$  with  $w_i = 1/(\delta x_i)^2$ . Note that the weighted average of the mass radii with different models obtained here is consistent with the result of the simultaneous fit to all the data sets.

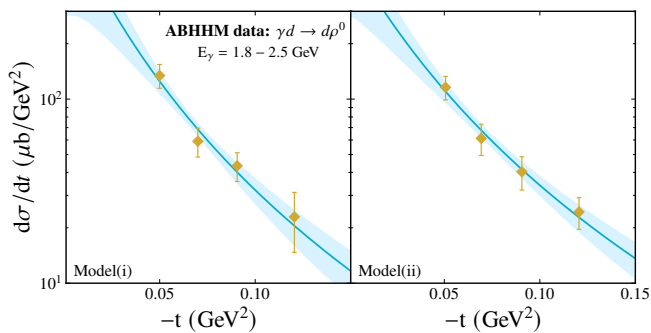


FIG. 1. The differential cross sections  $d\sigma/dt$  of near-threshold  $\rho^0$  meson photoproduction on the deuteron at  $E_\gamma = 1.8 - 2.5$  GeV. The solid curves show the fits of the scalar GFF model, where the cyan error band is derived from the uncertainties of the fitting parameters.

## B. Photoproduction of $\omega$ on deuteron

Y. Eisenberg *et al.* [33] have measured the coherent photoproduction of  $\omega$  in  $\gamma d$  interaction at  $E_\gamma = 4.3$  GeV. And the experiment was conducted by exposing the SLAC 40-inch bubble chamber to a quasi-monochromatic  $e^+$  annihilation photon beam with an energy of 4.3 GeV. Fig. 2 shows the differential cross sections of the near-threshold  $\omega$  photoproduction reaction  $\gamma d \rightarrow \omega d$  at  $E_\gamma = 4.3$  GeV. From the fits of the dipole GFF,  $\omega$  photoproduction differential cross-section data implies the deuteron mass radius to be  $2.04 \pm 0.47$  fm. The solid curves show the fits of the scalar GFF model, where the cyan error band is the uncertainty of fitting parameters. To quantify the quality of fit, the obtained dipole parameter  $m_s$  and the extracted deuteron radius  $\sqrt{\langle R_m^2 \rangle}$  from the differential cross sections of  $\omega$  photoproduction near threshold are listed in Table II.

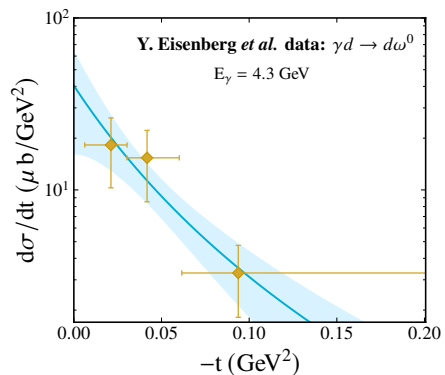


FIG. 2. The differential cross sections of the near-threshold  $\omega$  photoproduction on deuteron at  $E_\gamma=4.3$  GeV as a function of the momentum transfer  $-t$ . The experimental data points in the figure only show statistical errors. The solid curves show the fits of the scalar GFF, where the cyan error band is derived from the uncertainties of the fitting parameters.

$E_\gamma$ (GeV)	$m_s$ (GeV)	$\sqrt{\langle R_m^2 \rangle}$ (fm)
4.3	$0.33 \pm 0.08$	$2.04 \pm 0.47$

TABLE II. The extracted value of the dipole parameter  $m_s$  and deuteron mass radius  $\sqrt{\langle R_m^2 \rangle}$  from the differential cross-section data of  $\omega$  photoproduction near threshold at  $E_\gamma=4.3$  GeV, extrapolated to  $t = 0$  GeV<sup>2</sup>.

## C. Photoproduction of $\phi$ on deuteron

In our previous work [7], we analyzed the coherent  $\phi$ -photoproduction differential cross sections on deuterium target from CLAS and LEPS collaborations [34–37], obtaining a deuteron mass radius of  $1.95 \pm 0.19$  fm. This value is consistent with the values extracted from the current  $\rho^0$  and  $\omega$  meson analyses within the statistical uncertainties, strongly supporting the robustness and universality of our theoretical approach across different vector meson channels.

## D. Global analysis with $\rho^0$ , $\omega$ and $\phi$ photoproduction on deuteron

Combining three different vector meson near-threshold photoproduction channels, we performed a global analysis to obtain the average deuteron mass radius to be  $2.07 \pm 0.15$  fm, with the average dipole parameter to be  $m_s = 0.33 \pm 0.03$  GeV, which is more precise than the previous extraction using only the  $\phi$  meson photoproduction data. Fig. 3 shows the extracted deuteron mass radius as a function of the mass of the vector meson probe, where the vector meson arises from a photon fluctuating into a color dipole that subsequently interacts with the deuteron target.

The deuteron mass radii extracted by  $\rho^0$ ,  $\omega$  and  $\phi$  meson near-threshold photoproduction data are more or

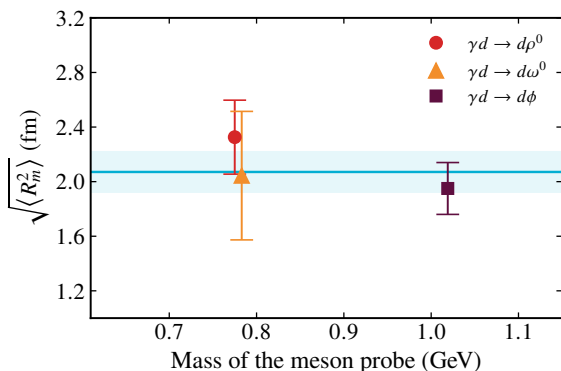


FIG. 3. The deuteron mass radii obtained from different vector meson near-threshold photoproduction processes. The solid cyan line and cyan color band in this figure show the average deuteron mass value and its uncertainty from the least-squares fit, respectively.

less consistent with each other. The  $\rho^0$  photoproduction data show a large mass radius than that from the  $\omega$  and  $\phi$  data. This may be due to the validity of applying the VMD model and the assumption of the scalar form factor with dipole form for the near-threshold light vector meson productions. Our findings strongly support the robustness of the VMD model and the dipole-form scalar GFF to characterize nuclear mass distributions. Future experiments at new and advanced facilities are anticipated to refine our analyses and further tests of the theoretical predictions.

#### IV. SUMMARY

Based on the assumptions of VMD model and a low energy QCD theorem, we extracted the deuteron mass radius by systematically analyzing different vector meson near-threshold photoproduction data. Utilizing a dipole parameterization of the scalar gravitational form factor within the VMD framework, the combined analysis of the three vector mesons  $\rho^0$ ,  $\omega$  and  $\phi$  photoproduction off the deuteron gives the average radius to be  $2.07 \pm 0.15$  fm, which is smaller than the world average of the deuteron charge radius ( $\text{CODATA-2020}$  evaluation gives deuteron charge radius  $2.1424 \pm 0.0021$  fm) [38, 39]. This result is in good agreement with the previous determination based solely on  $\phi$  photoproduction near-threshold data, thereby reinforcing the validity and universality of the adopted approach.

This analysis provides not only necessary constraints

for theoretical models of nuclear structure, but also a deeper understanding of the spatial distribution of mass within the deuteron. The consistent deuteron mass extracted from different near-threshold vector meson photoproduction data indicates that the VMD model combined with the dipole parameterization of the scalar GFF is a powerful tool to probe the internal structure of deuteron. In addition, precisely extracting the mass radius of deuteron is crucial for understanding the interplay between quark-gluon dynamics and nuclear binding, as well as for refining our knowledge of generalized parton distributions, which are closely related to GFF. Despite the success of our approach, several challenges remain. Currently, the approach to extracting the mass radius of deuterons parallels that of protons, meaning that the probe “sees” the structure of the entire nucleus without incorporating the shape of the deuteron itself into the size measurement process. Additionally, like the determination of the proton mass radius, different vector meson probes yield nearly identical deuteron mass radii within the uncertainty ranges, indicating that the form factor may not be sensitive to the type of meson probe used. The relatively large uncertainties in some of the individual channels highlights the necessity of improving experimental precision, especially in the low momentum-transfer region. Future experimental campaigns at next-generation electron scattering facilities and near-threshold photoproduction experiments are expected to provide high precision data, which will enable further improvement of the extraction of deuteron mass radius and a more detailed mapping of the internal mass distribution.

In short, our comprehensive analysis in different vector meson photoproduction channels contributes to a deeper understanding of the deuteron structure and lays a solid foundation for future theoretical and experimental investigations in nuclear mass radius physics. The ingenious extraction of the deuteron mass radius from various meson photoproduction processes highlights the prospect of combining advanced experimental techniques with rigorous theoretical modeling to reveal the complex structure of nuclear matter.

#### ACKNOWLEDGMENTS

This work is supported by the National Natural Science Foundation of China under the Grant NO. 12305127, the International Partnership Program of the Chinese Academy of Sciences under the Grant NO. 016GJHZ2022054FN. and National Key R&D Program of China under the Grant NO. 2024YFE0109802.

[1] R. e. a. Pohl, The size of the proton, *Nature* **466**, 213 (2010).

[2] A. Antognini *et al.*, Proton Structure from the Measurement of  $2S - 2P$  Transition Frequencies of

- Muonic Hydrogen, *Science* **339**, 417 (2013).
- [3] C. E. Carlson, The Proton Radius Puzzle, *Prog. Part. Nucl. Phys.* **82**, 59 (2015).
  - [4] J. M. Alarcón, D. W. Higinbotham, and C. Weiss, Precise determination of the proton magnetic radius from electron scattering data, *Phys. Rev. C* **102**, 035203 (2020), arXiv:2002.05167 [hep-ph].
  - [5] Y.-H. Lin, H.-W. Hammer, and U.-G. Meißner, High-precision determination of the electric and magnetic radius of the proton, *Phys. Lett. B* **816**, 136254 (2021), arXiv:2102.11642 [hep-ph].
  - [6] D. Djukanovic, G. von Hippel, H. B. Meyer, K. Ottnad, M. Salg, and H. Wittig, Precision Calculation of the Electromagnetic Radii of the Proton and Neutron from Lattice QCD, *Phys. Rev. Lett.* **132**, 211901 (2024), arXiv:2309.07491 [hep-lat].
  - [7] R. Wang, W. Kou, C. Han, J. Evslin, and X. Chen, Proton and deuteron mass radii from near-threshold  $\phi$ -meson photoproduction, *Phys. Rev. D* **104**, 074033 (2021), arXiv:2108.03550 [hep-ph].
  - [8] D. E. Kharzeev, Mass radius of the proton, *Phys. Rev. D* **104**, 054015 (2021).
  - [9] R. Wang, W. Kou, Y.-P. Xie, and X. Chen, Extraction of the proton mass radius from the vector meson photoproductions near thresholds, *Phys. Rev. D* **103**, L091501 (2021), arXiv:2102.01610 [hep-ph].
  - [10] C. Han, G. Xie, W. Kou, R. Wang, and X. Chen, The neutron and proton mass radii from the vector meson photoproduction data on the deuterium target, *Eur. Phys. J. A* **58**, 105 (2022), arXiv:2201.08535 [hep-ph].
  - [11] R. Wang, C. Han, and X. Chen, Exploring the mass radius of  $^4\text{He}$  and implications for nuclear structure, *Phys. Rev. C* **109**, L012201 (2024), arXiv:2309.01416 [hep-ph].
  - [12] I. Y. Kobzarev and L. B. Okun, GRAVITATIONAL INTERACTION OF FERMIONS, *Zh. Eksp. Teor. Fiz.* **43**, 1904 (1962).
  - [13] H. Pagels, Energy-Momentum Structure Form Factors of Particles, *Phys. Rev.* **144**, 1250 (1966).
  - [14] O. V. Teryaev, Gravitational form factors and nucleon spin structure, *Front. Phys. (Beijing)* **11**, 111207 (2016).
  - [15] M. V. Polyakov and P. Schweitzer, Forces inside hadrons: pressure, surface tension, mechanical radius, and all that, *Int. J. Mod. Phys. A* **33**, 1830025 (2018).
  - [16] X. Ji, Proton mass decomposition: naturalness and interpretations, *Front. Phys.* **16**, 64601 (2021).
  - [17] X. Ji, Gauge-Invariant Decomposition of Nucleon Spin, *Phys. Rev. Lett.* **78**, 610 (1997).
  - [18] V. D. e. a. Burkert, The pressure distribution inside the proton, *Nature* **557**, 396 (2018).
  - [19] W. e. a. Xiong, A small proton charge radius from an electron-proton scattering experiment, *Nature* **575**, 147 (2019).
  - [20] H.-W. Hammer and U.-G. Meißner, The proton radius: From a puzzle to precision, *Sci. Bull.* **65**, 257 (2020).
  - [21] R. Dupré, M. Guidal, and M. Vanderhaeghen, Tomographic image of the proton, *Phys. Rev. D* **103**, 014023 (2021).
  - [22] K. Kumerički, S. Liuti, and H. Moutarde, Phenomenological access to gravitational form factors of the nucleon, *JHEP* **10**, 063.
  - [23] G. A. Miller, Defining the proton radius: A unified treatment, *Phys. Rev. C* **99**, 035202 (2019), arXiv:1812.02714 [nucl-th].
  - [24] I. I. Strakovsky *et al.*, Photoproduction of the  $\omega$  meson on the proton near threshold, *Phys. Rev. C* **91**, 045207 (2015), arXiv:1407.3465 [nucl-ex].
  - [25] I. I. Strakovsky, L. Pentchev, and A. Titov, Comparative analysis of  $\omega p$ ,  $\phi p$ , and  $J/\psi p$  scattering lengths from A2, CLAS, and GlueX threshold measurements, *Phys. Rev. C* **101**, 045201 (2020), arXiv:2001.08851 [hep-ph].
  - [26] L. Pentchev and I. I. Strakovsky,  $J/\psi$ - $p$  Scattering Length from the Total and Differential Photoproduction Cross Sections, *Eur. Phys. J. A* **57**, 56 (2021), arXiv:2009.04502 [hep-ph].
  - [27] X.-Y. Wang, F. Zeng, and I. I. Strakovsky,  $\psi^{(*)}p$  scattering length based on near-threshold charmonium photoproduction, *Phys. Rev. C* **106**, 015202 (2022), arXiv:2205.07661 [hep-ph].
  - [28] C. Han, W. Kou, R. Wang, and X. Chen, Extraction of  $\omega n$ ,  $\omega p$ , and  $\phi N$  scattering lengths from  $\omega$  and  $\phi$  differential photoproduction cross sections on a deuterium target, *Phys. Rev. C* **107**, 015204 (2023), arXiv:2210.11276 [hep-ph].
  - [29] C. Han, W. Kou, R. Wang, and X. Chen, Vector meson-nucleon scattering length  $|\alpha_{VN}|$  and trace anomalous energy contribution to the nucleon mass  $T_A$ , *Eur. Phys. J. A* **59**, 118 (2023), arXiv:2211.17102 [hep-ph].
  - [30] W. Kou, R. Wang, and X. Chen, Determination of the gluonic gravitational form factors of the proton, *Phys. Rev. D* **103**, 014025 (2021).
  - [31] S. J. Brodsky, L. Frankfurt, J. F. Gunion, A. H. Mueller, and M. Strikman, Diffractive lepton production of vector mesons in QCD, *Phys. Rev. D* **50**, 3134 (1994), arXiv:hep-ph/9402283.
  - [32] P. Benz, O. Braun, H. Butenschön, D. Gall, U. Idschok, C. Kiesling, G. Knies, K. Müller, B. Nellen, R. Schiffer, P. Schlamp, H. J. Schnackers, P. Spiering, J. Stiewe, and F. Storim, Photoproduction of  $\rho^0$ ,  $\omega$  and  $\rho^-$  mesons on deuterons at energies between 1 and 5 GeV, *Nucl. Phys. B* **79**, 10 (1974).
  - [33] Y. Eisenberg, B. Haber, E. Kogan, E. E. Ronat, A. Shapira, and G. Yekutieli, Photoproduction of  $\rho^0$  and  $\omega$  in  $\gamma d$  interactions at 4.3 GeV, *Nucl. Phys. B* **38**, 349 (1972).
  - [34] H. Seraydaryan *et al.* (CLAS),  $\phi$ -meson photoproduction on Hydrogen in the neutral decay mode, *Phys. Rev. C* **89**, 055206 (2014), arXiv:1308.1363 [hep-ex].
  - [35] T. Mibe *et al.* (CLAS), First measurement of coherent phi-meson photoproduction on deuteron at low energies, *Phys. Rev. C* **76**, 052202 (2007), arXiv:nucl-ex/0703013.
  - [36] T. Mibe *et al.* (LEPS), Diffractive phi-meson photoproduction on proton near threshold, *Phys. Rev. Lett.* **95**, 182001 (2005), arXiv:nucl-ex/0506015.
  - [37] W. C. Chang *et al.*, Forward coherent phi-meson photoproduction from deuterons near threshold, *Phys. Lett. B* **658**, 209 (2008), arXiv:nucl-ex/0703034.
  - [38] P. Mohr, D. Newell, B. Taylor, and E. Tiesinga, CODATA Recommended Values of the Fundamental Physical Constants: 2022, (2024), arXiv:2409.03787 [hep-ph].
  - [39] R. Pohl *et al.* (CREMA), Laser spectroscopy of muonic deuterium, *Science* **353**, 669 (2016).